High temperature electron spin dynamics in bulk cubic GaN: Nanosecond spin lifetimes far above room-temperature

J. H. Bußß,[1] A. Schaefer,[1] T. Schupp,[2] D. J. As,[2] D. Hägele,[1] and J. Rudolph[1]
[1]*Arbeitsgruppe Spektroskopie der kondensierten Materie, Ruhr-Universität Bochum, Universitätsstraße 150, D-44780 Bochum, Germany*
[2]*Department of Physics, University of Paderborn, Warburger Str. 100, D-33095 Paderborn, Germany*

(Received 22 August 2014; accepted 26 October 2014; published online 4 November 2014)

The electron spin dynamics in *n*-doped bulk cubic GaN is investigated for very high temperatures from 293 K up to 500 K by time-resolved Kerr-rotation spectroscopy. We find extraordinarily long spin lifetimes exceeding 1 ns at 500 K. The temperature dependence of the spin relaxation time is in qualitative agreement with predictions of Dyakonov-Perel theory, while the absolute experimental times are an order of magnitude shorter than predicted. Possible reasons for this discrepancy are discussed, including the role of phase mixtures of hexagonal and cubic GaN as well as the impact of localized carriers. © *2014 AIP Publishing LLC*. [http://dx.doi.org/10.1063/1.4901108]

The continuously shrinking size of elementary device constituents like field-effect transistors has led to the enormous success of modern semiconductor electronics. New concepts will, however, soon be required to keep the tearing pace of improving performance, as projected by the International Technology Roadmap for Semiconductors. Spintronics[1] as a spin-based electronics envisions such improved device performance or innovative functionality by utilizing in addition the electron spin degree of freedom in, e.g., spin-transistors[2] or spin lasers.[3] A basic requirement for almost all spin-based device concepts is to maintain a non-equilibrium electron spin polarization. The efficient suppression of spin relaxation is, however, a challenging task, especially at high temperatures as required for applications. Possible routes to achieve slow spin relaxation include the control over the orbital motion of electrons via confinement[4] or localization[5] as well as the choice of suitable semiconductor materials, where the effectiveness of spin relaxation mechanisms depends critically on the semiconductor bandstructure. Generally, spin relaxation of mobile electrons is dominated by the Dyakonov-Perel (DP) mechanism[6] in III-V semiconductors, especially for high temperatures and *n*-type doping.[7] DP relaxation is caused by the combined action of momentum scattering and a spin-orbit coupling induced spin splitting of the conduction band occurring in semiconductors and semiconductor structures with broken inversion symmetry. The spin splitting acts like an effective, **k**-dependent magnetic field $\mathbf{\Omega}(\mathbf{k})$ on the electron spins. Random momentum scattering leads to a fluctuating effective magnetic field, which results in spin dephasing for an electron ensemble. The magnitude of $\mathbf{\Omega}(\mathbf{k})$ increases strongly with k, making DP relaxation very efficient for high temperatures. In the case of bulk III-V semiconductors, the conduction band spin splitting is an intrinsic material property. Small spin splittings are expected from $k \cdot p$-expressions[8] for weak spin-orbit coupling as witnessed by a small valence band spin-orbit splitting Δ_{so}, and for large bandgaps E_g. Based on these general trends, especially GaN with its small Δ_{so} and large E_g is expected to exhibit very small spin splittings and accordingly slow spin relaxation. The thermodynamically stable hexagonal phase of GaN (h-GaN) shows, however, fast spin relaxation due to its lower symmetry as compared to cubic semiconductors, which leads to an additional contribution to the spin splitting.[9–11] Only for the metastable cubic phase of GaN (c-GaN), which can be prepared under appropriate conditions,[12] slow electron spin relaxation was predicted[13,14] and experimentally demonstrated for low temperatures[15] and in a highly degenerate sample,[16] as well as in cubic GaN quantum dots.[17] There have been, however, no experimental investigations of electron spin relaxation in c-GaN for the regime of moderate *n*-type doping and high temperatures as relevant for potential applications. Temperature dependent measurements of electron spin relaxation in c-GaN as a material with presumably weak DP relaxation are in addition of fundamental interest to potentially unravel other mechanisms of spin relaxation, which are otherwise masked by fast DP relaxation in other semiconductor materials.[18]

Here, we experimentally investigate electron spin relaxation in moderately *n*-doped bulk c-GaN up to very high temperatures of 500 K by time-resolved Kerr-rotation (TRKR) spectroscopy. We find very long spin relaxation times up to the highest temperatures exceeding even 1 ns at 500 K.

The c-GaN epilayers investigated were grown by plasma-assisted molecular beam epitaxy.[12] A 580 nm-thick c-GaN layer was grown on a cubic AlN barrier with a thickness of 15 nm and 30 nm for sample A and B, respectively, on top of 3C-SiC substrates. The GaN layer was Si doped to a carrier density of $n_D = 1 \times 10^{18}\,\mathrm{cm}^{-3}$ for sample A, while sample B was intentionally undoped, resulting in a carrier density $n_D = 1 \times 10^{17}\,\mathrm{cm}^{-3}$ at room-temperature. The samples were mounted in vacuum in a dedicated high-temperature cell allowing for temperatures from 293 K to 500 K. A magnetic field B_{ext} was applied in the sample plane.

For the TRKR measurements, the setup as described in Ref. 19 was used. The energy of pump and probe beam was set to the maximum of the TRKR signal, shifting from 3.206 eV at 293 K to 3.113 eV at 500 K. The average power of pump and probe beam was 10 mW and 1 mW, respectively, for a pump spot of 100 μm diameter on the sample surface.

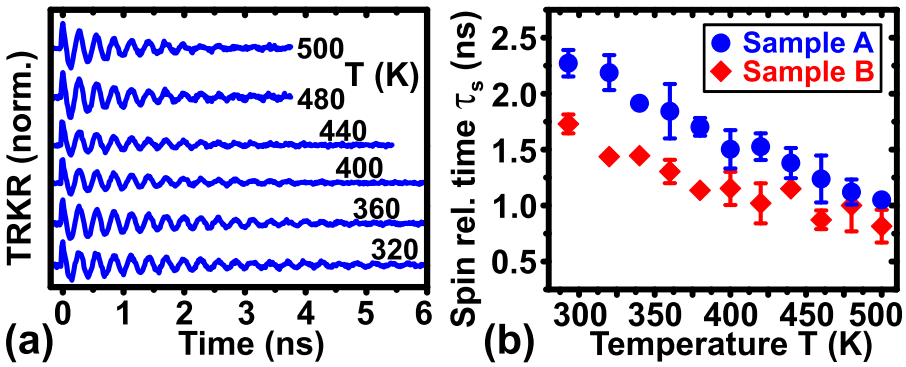

FIG. 1. (a) Normalized time-resolved Kerr-rotation transients for temperatures between $T = 320\,\mathrm{K}$ and 500 K for sample A in an external magnetic field $B_{\mathrm{ext}} = 0.1\,\mathrm{T}$. (b) Temperature dependence of the spin relaxation time τ_s for samples A and B at $B_{\mathrm{ext}} = 0.1\,\mathrm{T}$.

Figure 1(a) shows exemplarily TRKR transients of sample A for temperatures up to 500 K in an external magnetic field of $B_{\mathrm{ext}} = 0.1\,\mathrm{T}$. The transients already indicate slow spin relaxation up to 500 K as oscillations due to spin Larmor precession around the external magnetic field are still visible even after 2 ns. The transients are well fit by damped cosine fits of the form $[A_1 \exp(-t/\tau_c) + A_2] \exp(-t/\tau_s) \cos[\omega_L (t - t_0)]$ with τ_c as a carrier lifetime. The fits give the spin relaxation time τ_s and the Larmor precession frequency $\omega_L = \mathrm{g}_e \mu_B B_{\mathrm{ext}}/\hbar$ with the Landé-g-factor g_e. The extracted g_e-factor is compatible with the literature value[20] of $\mathrm{g}_e = 1.95$ for electrons in c-GaN, and it is found to be almost temperature independent and identical for both samples (not shown), indicating weak spin-orbit interaction.

The temperature dependence of spin relaxation as the main point of this work is shown in Fig. 1(b). The spin relaxation times of both sample A and B exhibit a very similar temperature dependence, characterized by a monotonic decrease for increasing temperature. Overall, we find very long spin relaxation times despite the high temperatures, even exceeding 1 ns at 500 K for sample A. In the following, we will compare the experimentally found spin relaxation times to theoretical predictions, starting with the DP mechanism as the generally dominating mechanism in bulk III-V semiconductors.

The main driving force of DP relaxation is the spin-orbit induced conduction band spin splitting, which is given by the Hamiltonian $H_{\mathrm{soc}} = \frac{\hbar}{2} \mathbf{\Omega}(\mathbf{k}) \cdot \boldsymbol{\sigma}$, with $\boldsymbol{\sigma}$ as the vector of Pauli spin matrices. $\mathbf{\Omega}(\mathbf{k})$ is in analogy to the Zeeman-Hamiltonian for electrons in an external magnetic field readily interpreted as an effective, $\mathbf{k}$-dependent magnetic field. The effective magnetic field $\mathbf{\Omega}^{\mathrm{D}}(\mathbf{k})$ for cubic semiconductors with zincblende structure is given by the cubic k^3-Dresselhaus[21] term

$$\Omega_i^{\mathrm{D}}(\mathbf{k}) = \frac{2\gamma_e}{\hbar} k_i \left(k_{i+1}^2 - k_{i+2}^2 \right), \tag{1}$$

with $i = x, y, z$ and γ_e as the spin splitting constant.

In the most basic approach to Dyakonov-Perel relaxation, the tensor γ_{ij} of spin relaxation rates is simply obtained by[22]

$$\gamma_{ij} = \frac{1}{2} \left(\delta_{ij} \langle \overline{\mathbf{\Omega}^2} \rangle - \langle \overline{\Omega_i \Omega_j} \rangle \right) \tau_p, \tag{2}$$

with the overbar denoting the angular average of $\mathbf{k}$, $\langle \ldots \rangle$ denoting the energetic average over the electronic momentum distribution, and τ_p as the averaged, effective momentum scattering time.

Here, the electronic momentum distribution can be approximated by a Boltzmann distribution as the Fermi temperatures $T_F^A = E_F^A/k_B = 282\,\mathrm{K}$ and $T_F^B = 61\,\mathrm{K}$ for sample A and B, respectively, are below the lattice temperature for the investigated temperature range. Carrying out the corresponding average, an isotropic spin relaxation tensor with the rate

$$\gamma_s = 1/\tau_s = 16 \gamma_e^2 m^{*3} (k_B T)^3 \tau_p / \hbar^8 \tag{3}$$

follows. The averaged, effective momentum scattering time τ_p has to be known for a comparison of the prediction of Eq. (3) to the experimental spin relaxation times τ_s. As τ_p could not be determined by transport measurements due to the highly conductive substrates, we model $\tau_p^{\mathrm{sim}} = \mu_{\mathrm{total}}^{\mathrm{sim}} m^*/e$ via the transport mobility $\mu_{\mathrm{total}}^{\mathrm{sim}}$, which combines the mobilities μ_{disl} due to scattering by dislocations,[23] μ_{pop} due to scattering with polar optical phonons,[24] μ_{dp} due to acoustic phonon deformation potential scattering,[25] μ_{ii} due to scattering with ionized impurities,[26] and μ_{pe} due to piezoelectric scattering[27] via Matthiessen's rule $1/\mu_{\mathrm{total}}^{\mathrm{sim}} = \sum_i 1/\mu_i$. Figures 2(a) and 2(b) show the simulated temperature dependence[28] of the total transport mobility $\mu_{\mathrm{total}}^{\mathrm{sim}}$ and the contributions of the individual scattering mechanisms for samples A and B, respectively, where we use a dislocation density $n_{\mathrm{disl}} = 5 \times 10^9\,\mathrm{cm}^{-2}$ typical for the thickness of the investigated samples.[29] Figures 2(c) and 2(d) demonstrate the influence of different dislocation densities from $n_{\mathrm{disl}} = 2 \times 10^9\,\mathrm{cm}^{-2}$ up to $2 \times 10^{10}\,\mathrm{cm}^{-2}$ on the mobility. These dislocation densities cover the range found for c-GaN on SiC[29] and result in a variation of the total mobility by approximately a factor of two around the mobility for the typical dislocation density. Overall, the simulated total mobility agrees well with experimental values for the mobility in c-GaN.[30–32] Scattering by polar optical phonons and by dislocations is found to clearly dominate in the investigated temperature range, with polar optical phonon scattering being dominant for temperatures $T > 350\,\mathrm{K}$.

Figure 3(a) compares the product $\tau_s \cdot \tau_p^{\mathrm{sim}}$ of the experimentally determined spin relaxation time τ_s and the modeled momentum scattering time τ_p^{sim} to the predicted inverse averaged effective magnetic field $1/\langle \Omega_{\mathrm{eff}}^2 \rangle \equiv \hbar^8/(16 \gamma_e^2 m^{*3} k_B^3 T^3)$ according to Eq. (3) on a double-logarithmic scale for different values of the dislocation density n_{disl}. For the spin splitting constant γ_e, the values $\gamma_e = 0.84\,\mathrm{eV\,\AA^3}$ and $\gamma_e = 0.235\,\mathrm{eV\,\AA^3}$, respectively, are used, corresponding to the spread of the theoretical values available from tight-binding calculations.[14,16,33]

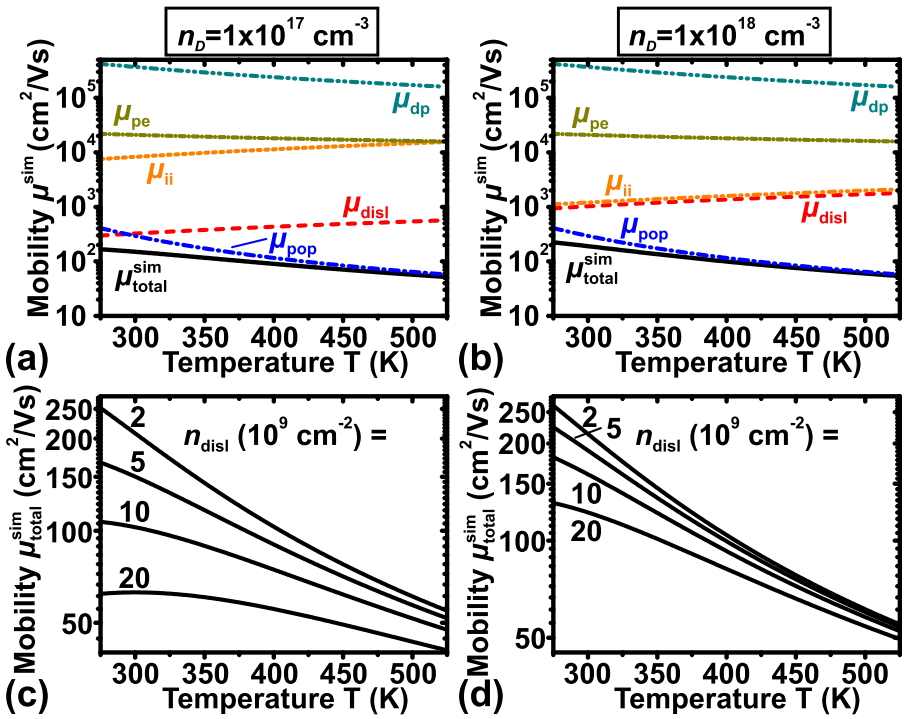

FIG. 2. Simulated temperature dependence of the total transport mobility μ^{sim}_{total} and the individual contributions to the mobility for a dislocation density $n_{disl} = 5 \times 10^9\,cm^{-2}$ and a carrier concentration of (a) $n_D = 1 \times 10^{17}\,cm^{-3}$ and (b) $n_D = 1 \times 10^{18}\,cm^{-3}$. Simulated temperature dependence of the total transport mobility μ^{sim}_{total} for different dislocation densities n_{disl} from $2 \times 10^9\,cm^{-2}$ to $2 \times 10^{10}\,cm^{-2}$ for (c) $n_D = 1 \times 10^{17}\,cm^{-3}$ and (d) $n_D = 1 \times 10^{18}\,cm^{-3}$.

While the slope of the temperature dependence is well reproduced, the predicted spin relaxation times are approximately one order of magnitude longer than the measured times even for the extreme assumption of the largest value for γ_e and the longest momentum scattering time τ_p^{sim} corresponding to the smallest dislocation density.

Though Eq. (2) has been successfully applied to the description of spin relaxation in GaN,[9–11,19] it is based on substantial approximations, neglecting, e.g., the different efficiencies and the energy dependence of the various momentum scattering mechanisms. A refined description of Dyakonov-Perel relaxation was given by Pikus and Titkov[8] starting from the energy dependent spin relaxation rate

$$\tilde{\gamma}_{ij}^{PT} = (\delta_{ij}\overline{\Omega^2} - \overline{\Omega_i\Omega_j})\left(\sum_i(\gamma_3^i/\tilde{\tau}_p^i)\right)^{-1}, \qquad (4)$$

summing over the energy dependent momentum scattering times $\tilde{\tau}_p^i$ of the different scattering mechanisms weighted by their efficiency factors γ_3^i. Carrying out the angular average and using again a Boltzmann distribution for the electron momenta, the spin relaxation rate

$$\gamma_s^{PT} = \frac{8\gamma_e^2(m^*k_BT)^3}{\hbar^8}\left(\sum_i\frac{1}{Q_i\tau_p^i}\right)^{-1} = \frac{\langle\Omega_{eff}^2\rangle}{2}(\tau_pQ)_{total} \qquad (5)$$

follows, with $\langle\Omega_{eff}^2\rangle$ as defined above, $(\tau_pQ)_{total} \equiv (\sum_i 1/\tau_p^iQ_i)^{-1}$, $\tau_p^i = \langle\tilde{\tau}_p^iE_k\rangle/\langle E_k\rangle$ and[8] $Q_i = 16[\nu+(7/2)][\nu+(5/2)]/(35\gamma_3^i)$ as efficiency coefficients, which have been introduced assuming a power law $\tilde{\tau}_p \propto E_k^\nu$ for the individual scattering mechanisms. The above simulations of the mobility allow to identify the contributions from the different scattering mechanisms and to weight them with their corresponding efficiency factor. In the following, only scattering by polar optical phonons and by dislocations is considered according to the above discussion of the importance of the individual scattering mechanisms. The efficiency factor $\gamma_3^{pop} = 11/6$ gives $Q_{pop} \approx 3$ for scattering by polar optical phonons,[34] while we find $Q_{disl} = 32/21$ for scattering by the charge field of a dislocation

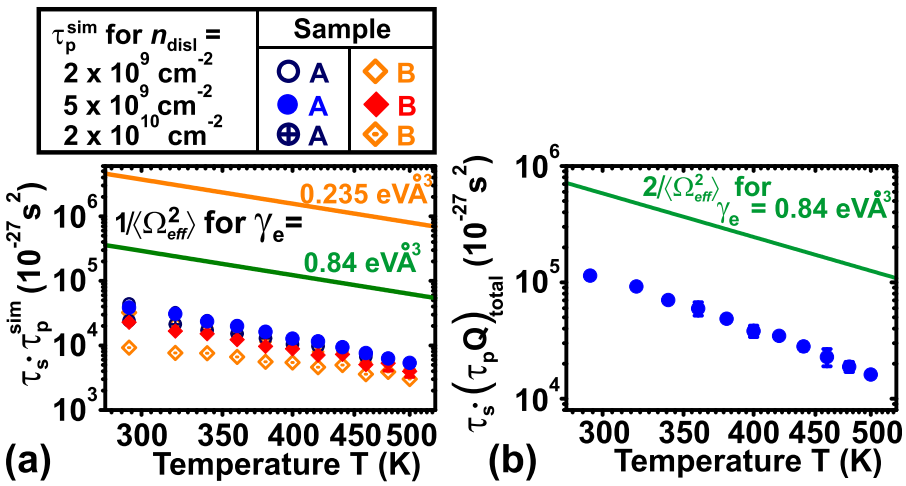

FIG. 3. (a) Temperature dependence of the product of spin relaxation time τ_s and the simulated momentum scattering time τ_p^{sim} for samples A and B for different dislocation densities n_{disl}. The solid lines show the inverse averaged effective magnetic field $1/\langle\Omega_{eff}^2\rangle$ for different values of the spin splitting constant γ_e. (b) Temperature dependence of the product of spin relaxation time τ_s and the simulated momentum scattering time $(\tau_pQ)_{total}$ weighted by the efficiency coefficients for sample A for a dislocation density $n_{disl} = 5 \times 10^9\,cm^{-2}$. The solid line shows the inverse averaged effective magnetic field $2/\langle\Omega_{eff}^2\rangle$ for $\gamma_e = 0.84\,eV\,Å^3$.

using[35] $\gamma_3^{\mathrm{disl}}=6$ and $\tilde{\tau}_p^{\mathrm{disl}} \propto E_k^{3/2}$. The comparison of the product $\tau_s \cdot (\tau_p Q)_{\mathrm{total}}$ to $2/\langle \Omega_{\mathrm{eff}}^2 \rangle$ as predicted by Eq. (5) shows a slight improvement as compared to the simple approach of Eq. (3) [cf. Fig. 3(b)]. The experimental spin relaxation times are, however, still almost an order of magnitude shorter than theoretically predicted.

In the following, we will discuss possible reasons for the observed discrepancy between the experimentally found spin relaxation times and the predictions of DP theory as presented above. One obvious reason for the overestimation of spin relaxation times by DP theory could be a too small value of the spin splitting parameter γ_e. We note that the determination of γ_e is notoriously difficult, as is well-known also for the case of the thoroughly studied GaAs,[36] and no experimental value for γ_e is available for c-GaN. The available theoretical values[14,33,37] for γ_e show considerable scatter from $\gamma_e = 0.235\,\mathrm{eV\AA^3}$ to $0.84\,\mathrm{eV\AA^3}$, with, however, a tendency to smaller values of γ_e for increased accuracy of the calculations.[33] A too small value of the simulated mobility could also account for the gap between the experimental and the predicted spin relaxation times. The simulations seem, however, to rather slightly overestimate the mobilities as compared to available experimental values in c-GaN.[30–32] Another possible reason for the observed discrepancy is the assumption of an ideal, homogeneous bulk c-GaN crystal in the prediction of γ_e and the above discussion of DP relaxation. The real microstructure of c-GaN layers prepared under conditions completely analogous to the investigated c-GaN samples is, however, highly complex with possibly large impact on the spin dynamics.[29,38] Stacking faults on {111} crystallographic planes lead to inclusions of the thermodynamically stable h-GaN phase in the c-GaN matrix, with increasing hexagonal content for increasing layer thickness. Moreover, c-GaN epitaxial films on 3 C-SiC substrates show distinct anti-phase domains (APD) with different h-GaN content in the two types of APDs.[38] An influence of this phase mixture on the spin relaxation can be expected, e.g., by the polar faces of the h-GaN inclusions acting as a random Rashba field similar to the random Rashba field of dopant ions.[39] In addition, the very effective DP spin relaxation in the polar h-GaN inclusions[9–11] might contribute to the observed spin relaxation via thermally activated scattering between the cubic and hexagonal phases. Furthermore, photoluminescence and micro-Raman measurements indicate inhomogeneous microstrain distributions in the c-GaN layers.[31,38,40] Such microstrain variations might contribute to spin relaxation via strain-induced conduction band spin splittings.[41]

In general, also the Elliott-Yafet (EY) and the Bir-Aronov-Pikus (BAP) mechanism contribute to the spin relaxation of mobile electrons.[42] The spin relaxation time due to the EY mechanism can, however, be estimated by expressions[27,42] for the long-range part to be on the order of μs in c-GaN. The EY mechanism does therefore not contribute significantly to spin relaxation in c-GaN. The BAP mechanism requires substantial hole concentrations and is generally found to be ineffective for *n*-doped samples at elevated temperatures.[7,42] Hence, it is not expected to play a role in the investigated c-GaN samples. Spin relaxation of localized electrons via the hyperfine interaction (HF) with nuclei could, however, be important here, with efficient spin exchange between the localized and mobile electrons leading to spin relaxation also for the system of mobile electrons.[19] Such HF mediated spin relaxation was just recently demonstrated in c-GaN at low temperatures.[43] Electrons deeply localized at states like deep defects or donor states with an activation energy[30] of 160 meV and 600 meV, respectively, in c-GaN might, however, certainly contribute to spin relaxation even at the high temperatures investigated here. The magnetic field dependence of the spin relaxation rate γ_s of sample A at room temperature supports this point, as it shows a weak $\gamma_s \propto B_{\mathrm{ext}}$ dependence (not shown) as being typical for the spin relaxation of localized electrons.[19]

In conclusion, we investigated electron spin relaxation in moderately *n*-doped cubic GaN at very high temperatures up to 500 K. We find extraordinarily long spin relaxation times even exceeding 1 ns at 500 K, making cubic GaN a highly interesting material system for possible spintronics applications. The temperature dependence of spin relaxation is in qualitative agreement with Dyakonov-Perel theory, which, however, predicts an order of magnitude longer spin relaxation times. Possible reasons for this discrepancy are discussed, including the role of hexagonal GaN inclusions and of localized electrons.

We gratefully acknowledge financial support by the German Science Foundation (DFG priority program 1285 "Semiconductor Spintronics" and DFG graduate program GRK 1464 "Micro- and Nanostructures in Optoelectronics and Photonics").

[1]*Semiconductor Spintronics and Quantum Computation*, edited by D. D. Awschalom and N. Samarth (Springer-Verlag, Berlin, 2002).
[2]S. Sugahara and J. Nitta, Proc. IEEE **98**, 2124 (2010).
[3]M. Holub, J. Shin, D. Saha, and P. Bhattacharya, Phys. Rev. Lett. **98**, 146603 (2007).
[4]Y. Ohno, R. Terauchi, T. Adachi, F. Matsukura, and H. Ohno, Phys. Rev. Lett. **83**, 4196 (1999).
[5]M. Paillard, X. Marie, P. Renucci, T. Amand, A. Jbeli, and J. M. Gérard, Phys. Rev. Lett. **86**, 1634 (2001).
[6]M. I. Dyakonov and V. I. Perel, Sov. Phys. Solid State **13**, 3023 (1972).
[7]J. H. Jiang and M. W. Wu, Phys. Rev. B **79**, 125206 (2009).
[8]*Optical Orientation*, edited by F. Meier and B. P. Zakharchenya (North-Holland, Amsterdam, 1984).
[9]J. H. Buß, J. Rudolph, F. Natali, F. Semond, and D. Hägele, Appl. Phys. Lett. **95**, 192107 (2009).
[10]J. H. Buß, J. Rudolph, F. Natali, F. Semond, and D. Hägele, Phys. Rev. B **81**, 155216 (2010).
[11]J. H. Buß, J. Rudolph, S. Starosielec, A. Schaefer, F. Semond, Y. Cordier, A. D. Wieck, and D. Hägele, Phys. Rev. B **84**, 153202 (2011).
[12]D. J. As, in *III-Nitride Semiconductor Materials: Growth*, edited by M. O. Manasreh and I. T. Ferguson (Taylor and Francis, New York, 2003); D. J. As, S. Potthast, J. Schörmann, S. F. Li, K. Lischka, H. Nagasawa, and M. Abe, Mater. Sci. Forum **527**, 1489 (2006).
[13]S. Krishnamurthy, M. van Schilfgaarde, and N. Newman, Appl. Phys. Lett. **83**, 1761 (2003).
[14]Z. G. Yu, S. Krishnamurthy, M. van Schilfgaarde, and N. Newman, Phys. Rev. B **71**, 245312 (2005).
[15]A. Tackeuchi, H. Otake, Y. Ogawa, T. Ushiyama, T. Fujita, F. Takano, and H. Akinaga, Appl. Phys. Lett. **88**, 162114 (2006).
[16]J. H. Buß, J. Rudolph, T. Schupp, D. J. As, K. Lischka, and D. Hägele, Appl. Phys. Lett. **97**, 062101 (2010).
[17]D. Lagarde, A. Balocchi, H. Carrère, P. Renucci, T. Amand, X. Marie, S. Founta, and H. Mariette, Phys. Rev. B **77**, 041304 (2008).
[18]S. Oertel, J. Hübner, and M. Oestreich, Appl. Phys. Lett. **93**, 132112 (2008).

[19]J. H. Buß, J. Rudolph, S. Shvarkov, H. Hardtdegen, A. D. Wieck, and D. Hägele, Appl. Phys. Lett. **102**, 192102 (2013).
[20]M. W. Bayerl, M. S. Brandt, T. Graf, O. Ambacher, J. A. Majewski, M. Stutzmann, D. J. As, and K. Lischka, Phys. Rev. B **63**, 165204 (2001).
[21]G. Dresselhaus, Phys. Rev. **100**, 580 (1955).
[22]D. Hägele, S. Döhrmann, J. Rudolph, and M. Oestreich, Adv. Solid State Phys. **45**, 253 (2005).
[23]B. Pödör, Phys. Status Solidi B **16**, K167 (1966).
[24]R. L. Petritz and W. W. Scanlon, Phys. Rev. **97**, 1620 (1955).
[25]J. Bardeen and W. Shockley, Phys. Rev. **80**, 72 (1950).
[26]D. Chattopadhyay and H. J. Queisser, Rev. Mod. Phys. **53**, 745 (1981).
[27]P. H. Song and K. W. Kim, Phys. Rev. B **66**, 035207 (2002).
[28]Material parameter used in the simulations: $m^* = 0.15\,m_0$, $\varepsilon_s = 9.5$, $\varepsilon_\infty = 5.35$, $a = 4.5$ Å, $T_{LO} = 1065$ K, $a_c = 2.77$ eV, $c_{11} = 296$ GPa, $c_{12} = 154$ GPa, $c_{44} = 206$ GPa, and $e_{14} = 0.5$ C/m^2.
[29]D. J. As and K. Lischka, in *Nonpolar Cubic III-Nitrides: From the Basics of Growth to Device Applications*, edited by M. Henini (Elsevier, Oxford, 2013).
[30]D. J. As, D. Schikora, A. Greiner, M. Lübbers, J. Mimkes, and K. Lischka, Phys. Rev. B **54**, R11118 (1996).
[31]O. Brandt, in *Group III Nitride Semiconductor Compounds*, edited by B. Gil (Clarendon Press, Oxford, 1998).
[32]M. Kohno, T. Nakamura, T. Kataoka, R. Katayama, and K. Onabe, Phys. Status Solidi C **5**, 1805 (2008); J. N. Kuznia, J. W. Yang, Q. C. Chen, S. Krishnankutty, M. A. Khan, T. George, and J. Frietas, Appl. Phys. Lett. **65**, 2407 (1994); H. Okumura, S. Misawa, T. Okahisa, and S. Yoshida, J. Cryst. Growth **136**, 361 (1994); S. V. Novikov, N. M. Stanton, R. P. Campion, R. D. Morris, H. L. Geen, C. T. Foxon, and A. J. Kent, Semicond. Sci. Technol. **23**, 015018 (2008).
[33]K. Shen, J. Fu, and M. Wu, Solid State Commun. **151**, 1924 (2011).
[34]Here we corrected for several misprints in the English version of the corresponding section of Ref. 8, including the correct value of γ_3^{pop} and inconsistent use of γ_3.
[35]D. Jena, Phys. Rev. B **70**, 245203 (2004).
[36]See supplementary material in J. J. Krich and B. I. Halperin, Phys. Rev. Lett. **98**, 226802 (2007) for a compilation of theoretical and experimental values of γ_e for GaAs.
[37]J. Y. Fu and M. W. Wu, J. Appl. Phys. **104**, 093712 (2008).
[38]R. M. Kemper, T. Schupp, M. Häberlen, T. Niendorf, H.-J. Maier, A. Dempewolf, F. Bertram, J. Christen, R. Kirste, A. Hoffmann, J. Lindner, and D. J. As, J. Appl. Phys. **110**, 123512 (2011).
[39]V. I. Melnikov and E. I. Rashba, Sov. Phys. JETP **34**, 1353 (1972); E. Y. Sherman, Appl. Phys. Lett. **82**, 209 (2003).
[40]R. Klann, O. Brandt, H. Yang, H. T. Grahn, K. Ploog, and A. Trampert, Phys. Rev. B **52**, R11615 (1995).
[41]M. I. Dyakonov, V. A. Marushchak, V. I. Perel, and A. N. Titkov, Sov. Phys. JETP **63**, 655 (1986).
[42]M. W. Wu, J. H. Jiang, and M. Q. Weng, Phys. Rep. **493**, 61 (2010).
[43]G. Wang, C. R. Zhu, B. L. Liu, H. Ye, A. Balocchi, T. Amand, B. Urbaszek, H. Yang, and X. Marie, Phys. Rev. B **90**, 121202 (2014).